



# Exploring the role of aquaporin proteins in the pre-protective action of Sanwei sandalwood decoction from adriamycin-induced chronic heart failure: A mechanistic study

Surilige<sup>a,\*\*</sup>, Pengfei Hu<sup>a</sup>, Tingting Bai<sup>c</sup>, Zhi Xiu<sup>b</sup>, Huijiya<sup>b</sup>, Ming Li<sup>b</sup>, Qingshan Zhang<sup>a</sup>, Quan Wan<sup>a,\*</sup>

<sup>a</sup> Affiliated Hospital of Inner Mongolia University for Nationalities Inner Mongolia, China

<sup>b</sup> Clinical Medical College of Inner Mongolia University for Nationalities Inner Mongolia, China

<sup>c</sup> Key Laboratory of Mongolian Medicine Pharmacology for Cardio Inner Mongolia, China

## ARTICLE INFO

### Keywords:

Sanwei sandalwood decoction  
Aquaporin proteins  
Network pharmacology  
Molecular docking technology  
Adriamycin-induced chronic heart failure

## ABSTRACT

This study employed network pharmacology, molecular docking technology, and modern pharmacological research methods to explore the pre-protective effect and underlying mechanism, Sanwei sandalwood decoction, against Adriamycin-induced Chronic Heart Failure, with a particular focus on the involvement of aquaporins. Additionally, the study highlighted aquaporins as a significant factor, affecting processes such as cell proliferation and response to reactive oxygen species. The results of *in vivo* experiments demonstrated that the administration of Sanwei sandalwood decoction in rats with chronic heart failure led to an enhancement in the ejection fraction and improved heart ejection function. Additionally, the decoction significantly reduced the serum levels of Creatine Kinase, Creatine Kinase-MB, and N-terminal pro-B-type natriuretic peptide. Furthermore, the relative expression of Aquaporin-1, 4, and 7mRNAs and proteins in the hearts of rats with chronic heart failure was down-regulated upon treatment. Overall, Sanwei sandalwood decoction can have an effective cardioprotective effect in preventing Adriamycin-induced Chronic Heart Failure in rats.

## 1. Introduction

Adriamycin (doxorubicin, Dox) is a potent chemotherapy drug belonging to the anthracycline class. It is widely used as a first-line treatment for breast cancer and gastrointestinal tract tumors due to its broad-spectrum effectiveness. However, one of its major drawbacks is its association with Chronic Heart Failure. Numerous studies have revealed that the incidence of heart failure increases with cumulative doses of Dox. At doses up to 400 mg/m<sup>2</sup>, the occurrence of heart failure is approximately 5 %, which rises to approximately 17 % at cumulative doses of 550 mg/m<sup>2</sup> [1]. The cardiotoxic mechanism primarily involves the production of harmful reactive oxygen species (ROS) like hydrogen peroxide (H<sub>2</sub>O<sub>2</sub>) and superoxide anion (O<sub>2</sub><sup>-</sup>) through the chelation of iron ions by anthracyclines. This generation of ROS causes lipid peroxidation of cardiomyocyte membranes, resulting in myocardial injury [2]. Chronic heart failure (CHF) represents the advanced stage of various heart diseases, characterized by impaired ventricular filling

\* Corresponding author.

\*\* Corresponding author.

E-mail addresses: [Surilige0475@163.com](mailto:Surilige0475@163.com) (Surilige), [wanquan120@126.com](mailto:wanquan120@126.com) (Q. Wan).

<https://doi.org/10.1016/j.heliyon.2023.e22718>

Received 9 August 2023; Received in revised form 16 November 2023; Accepted 16 November 2023

Available online 25 November 2023

2405-8440/© 2023 The Authors. Published by Elsevier Ltd. This is an open access article under the CC BY-NC-ND license (<http://creativecommons.org/licenses/by-nc-nd/4.0/>).

and/or ejection function. This condition leads to inadequate cardiac output to meet the metabolic demands of the body's tissues, resulting in a range of complex syndromes that seriously threaten global human health. Epidemiological surveys indicate that there are approximately 22.5 million CHF patients worldwide, with a prevalence of 2 %–3 % in Europe and a projected prevalence exceeding 25 % in the U.S. by 2030 [3,4]. As the global population ages, the number of elderly CHF patients is increasing, leading to a further rise in CHF prevalence, hospitalization rates, and medical expenses [5]. Therefore, effectively preventing and treating CHF, reducing morbidity and mortality rates, and enhancing the prognosis and quality of life for patients have become urgent global public health challenges. Addressing these issues is of paramount importance in the face of the aging population and the growing burden of CHF on healthcare systems worldwide.

Aquaporins (AQPs) are a group of transmembrane proteins that facilitate the movement of water and certain small molecules, such as heavy metals, chlorides and ammonia, across cell membranes in response to osmotic pressure differences or concentration gradients. In mammals, there are 13 different isoforms of AQPs, and in both human and rat hearts, AQP protein isoforms including AQPs-1, 4, and 7 are co-expressed [6]. AQPs are integral in the regulation of cardiac water-fluid metabolism, both in normal physiological conditions and during pathological states [7]. They work in coordination with ion channel substrate transporter proteins and phospholipid bilayers on cardiomyocyte membranes to maintain the balance of water-liquid metabolism in the myocardial interstitium and within cardiomyocytes [8]. Additionally, AQPs not only serve as channels for water and solute transport but also indirectly influence cardiac electrophysiological activities by modulating the ionic composition of cytosol and extracellular fluids, thereby affecting cardiac function [9]. It is evident that the expression levels of cardiac AQPs significantly influence water-liquid metabolism and cardiac function.

Sanwei sandalwood decoction (SWTX) is a basic formula utilized in Mongolian and Tibetan medicine to treat cardiovascular ailments. It comprises three herbs: jujube (*choerospondiatis fructus*), myristicae semen, and sandalwood (*santali albi lignum*), with jujube being the main ingredient in the formula. Guangzao, one of the constituents, contains phenolic acid, flavonoids, amino acids, and ravines, commonly used to address issues like "qi" stagnation, palpitations, shortness of breath, and anxiety, exhibiting certain heart-healthy effects [10]. Research has indicated that the total flavonoids in guangzao have a notable impact on improving arrhythmia in rats and can significantly enhance heart pumping function [11]. The formula's properties involve clearing heat, dispelling wind, and nourishing the heart, making it a frequently used treatment for cardiac fever in Mongolian and Tibetan medicine [12]. To study the mechanism of action of Chinese herbal formulas, network pharmacology and molecular docking are adopted, along with the distinctive characteristics of Chinese medicine, and ensuring accuracy and feasibility. In this study, we integrated the aforementioned methods with modern pharmacological research techniques to explore the role of AQPs in the pre-protective effect and mechanism of SWTX in countering Adriamycin Chronic Heart Failure.

## 2. Materials and methods

### 2.1. Collection and screening of active ingredients

We conducted a comprehensive analysis of the chemical constituents present in each herbal medicine of SWTX, which includes sandalwood, nutmeg, and guangzao. For data collection, we utilized the TCMSP database, a valuable resource for traditional Chinese medicine information. To assess the activity of the compounds, we employed two essential indicators, oral bioavailability (OB), and drug-likeness (DL), which are commonly used in drug screening processes. Specifically, we focused on active ingredients with an OB of at least 30 % and DL score of at least 0.18. Utilizing the TCMSP database, we screened the active ingredients of three traditional Chinese medicines: guangzao, nutmeg, and Bai Tan Xiang, to finalize the set of active ingredients for SWTX. For data analysis and processing, specific software and the TCMSP database were utilized, as depicted in Table 1.

### 2.2. Prediction of active ingredient targets

Using the TCMSP database, we retrieved the active ingredients that were previously screened. Next, we conducted a search to

**Table 1**  
Involved database and related analysis platform in the study.

NO.	Name	Wet	Version
1	TCMSP	<a href="http://lsp.nwu.edu.cn/tcmsp.php">http://lsp.nwu.edu.cn/tcmsp.php</a>	2.3
2	UniProt	<a href="https://www.uniprot.org">https://www.uniprot.org</a>	2020.05.05
3	GeneCards	<a href="https://www.genecards.org">https://www.genecards.org</a>	5.0
4	OMIM	<a href="https://omim.org/">https://omim.org/</a>	2020.05.05
5	TTD	<a href="http://db.idrblab.net/ttd/">http://db.idrblab.net/ttd/</a>	2020.06.01
6	Cytoscape	<a href="http://www.cytoscape.org/">http://www.cytoscape.org/</a>	3.7.2
7	STRING	<a href="https://string-db.org/">https://string-db.org/</a>	11.0
8	R	<a href="https://www.r-project.org/">https://www.r-project.org/</a>	3.6.2
9	PDB	<a href="http://www.rcsb.org">http://www.rcsb.org</a>	2020.05.05
10	PyMOL	<a href="https://pymol.org/2">https://pymol.org/2</a>	1.7.2.1
11	AutoDockTools	<a href="http://autodock.scripps.edu/resources/adt">http://autodock.scripps.edu/resources/adt</a>	1.5.6
12	Autodock vina	<a href="http://vina.scripps.edu">http://vina.scripps.edu</a>	1.1.2

identify the corresponding target proteins of these active ingredients. For this purpose, we utilized the Uniprot database to query the gene names corresponding to the target proteins. To consolidate the information, we merged the obtained target gene names and removed any duplicates. The resulting set of target gene names represents the targets of the active ingredients present in SWTX.

### 2.3. Collection of heart failure-related targets

The keyword “heart failure” was used to conduct searches for CHF-related targets in Gene Cards, OMIM, and TTD databases. The retrieved results from each database were then combined, and any duplicates were eliminated. After combining the results from the three databases and removing duplicates, the final set of targets obtained represented the relevant targets of CHF.

### 2.4. Prediction of potential targets and construction of “active ingredient-target” network

To identify potential targets of SWTX in treating CHF, Venn packages were employed to determine the common targets shared between SWTX and CHF. By mapping the intersection of these targets, the potential molecular targets crucial for SWTX’s therapeutic effects on CHF could be pinpointed. Subsequently, we used Cytoscape software to create a comprehensive active ingredient-target network diagram for SWTX. To further identify the responsible key active ingredients, we employed the degree value, a network analysis metric. By evaluating the degree value of each active ingredient in the network, we were able to prioritize the most significant components that play a pivotal role in SWTX’s effectiveness for CHF treatment.

### 2.5. Protein interaction network construction

To gain deeper insight into the mechanism of action of SWTX in treating CHF, the intersecting genes, obtained earlier through Venn package analysis, were imported into the STRING database. For a more focused analysis, the study species was limited to “Homo Sapiens”. To ensure the reliability of the protein-protein interactions (PPIs), the linkage score threshold was set to  $>0.9$ . The results of the PPI analysis were imported into Cytoscape software, where the interactions were visualized using the “NetworkAnalyzer” tool by constructing a PPI network. Nodes were identified based on having an average degree greater than two times, as these nodes represent central proteins with a higher number of interactions in the PPI network.

### 2.6. Molecular docking validation

To investigate the interactions between key active ingredients of SWTX and key targets, molecular docking validation was performed for both. Initially, the ChemOffice software was used to create the 3D structures of the key active ingredients. Subsequently, the 3D structures of the key targets were obtained from the Protein Data Bank (PDB) database, and PyMOL software was employed to prepare the proteins by dehydrating and dephosphorylating them. To facilitate the docking process, the Auto Dock 1.5.6 software converted the resulting protein files from pdb format to pdbqt format, and active pockets were identified. Then, the Vina script was executed to perform the docking process. A binding energy of less than 0 indicates spontaneous binding of the ligand and receptor. To assess the reliability of the prediction of bioinformatic analysis, a binding energy threshold of  $\leq -5.0$  kJ/mol was adopted based on literature reports [7]. This criterion served as the basis for screening and evaluating the potential interactions between the active ingredients and targets.

### 2.7. Enrichment analysis

GO and KEGG pathway enrichment analyses were performed using ClusterProfiler, along with the org. Hs.eg.db package, enrichplot, and ggplot2 package, the results were visualized using these packages to provide a comprehensive and clear representation of the enriched biological processes and pathways associated with the data.

### 2.8. Kyoto encyclopedia of genes and genomes relationship network construction

Based on the signaling pathways obtained in Section 2.7, a “key target-signaling pathway” relationship network was obtained. This network was imported into Cytoscape software to visualize and analyze the relationships between key targets and their associated signaling pathways. From this network, the 20 most significantly enriched pathways were selected and mapped onto the KEGG network.

### 2.9. Experimental animals and modeling methods

Healthy male Sprague-Dawley rats of specific pathogen-free (SPF) class, and weighing  $180 \pm 20$ g, were provided by Liaoning Changsheng Laboratory Animal Co. These rats were housed in SPF classrooms at the Experimental Animal Centre of Inner Mongolia University of Nationalities, where conditions included a humidity range of 45 %–55 %, a temperature of  $23 \pm 0.5$  °C, and alternating day and night cycles. The rats were given free access to water and food throughout the study. All animal experiments were conducted in strict accordance with the guidelines and regulations of the Animal Ethics Committee of Inner Mongolia University for Nationalities.

After a period of acclimatization, the rats were randomly assigned to one of three groups: the blank group, the model group, or the

SWTX group (referred to as the treatment group), with 10 rats in each group. Rats in the treatment group were administered SWTX orally at a dose of 2 g/kg daily for 15 consecutive days. In contrast, rats in the blank and model groups received an equivalent volume of saline as a control [13]. Two weeks later, rats in the blank group were injected intraperitoneally with saline once a week. To induce CHF, the remaining rats received injections of doxorubicin (diluted in saline to a concentration of 2 mg/mL) at a dose of 1.5 mL/kg once a week for five weeks. The combined dosage of 21 mg/kg was used to establish the model, following the methodology outlined in relevant literature [14].

### 2.10. General indicator monitoring

Throughout the entire experimental period, starting from the first week of modeling until the end of the seventh week of administration, the weight of each rat group was recorded using the same electronic scale. Statistical analysis was conducted on the weight data for seven consecutive weeks.

### 2.11. Histopathological analysis

The heart of rats were immobilized using a 4 % paraformaldehyde solution. Subsequently, appropriate-sized tissue samples were taken, and any residual paraformaldehyde on the surface was washed away with water. The tissues were then dehydrated and embedded in paraffin wax, followed by sectioning into slices with a thickness of 4–5  $\mu\text{m}$ . The obtained slides were carefully retrieved and baked at 60 °C for 1–2 h. Afterward, the slides were dewaxed using xylene and then rehydrated with various concentrations of ethanol. To visualize the nuclei and cytoplasm, the slides were stained following the instructions provided in the hematoxylin-eosin staining kit.

### 2.12. Creatine kinase, creatine kinase-MB, and lactate dehydrogenase levels of activity assay

We assessed the levels of creatine kinase (CK), creatine kinase-MB (CK-MB), and lactate dehydrogenase (LDH) activity in rat serum using commercially available enzyme-linked immunosorbent assay (ELISA) kits (Jiangsu Zeyu Biotechnology Co., Jiangsu, China).

### 2.13. Ultrasonography of cardiac function in rats

Rats were administered an intraperitoneal injection of 7 % chloral hydrate at a dose of 0.3 ml per 100 g of body weight for anesthesia. Once anesthetized, the rats were placed in a supine position and securely fixed on an electrode plate. The chest area was then depilated, and a medical ultrasound coupling agent was evenly applied to the thoracic region. The left ventricle was located, and the position of the measurement line was determined at the posterior edge of the papillary muscle. Various parameters related to the rat's heart were measured to assess cardiac function, including the thickness of the left ventricular diastasis anterior wall (LVSD), the left ventricular end-diastolic dimension (LVIDd), the left ventricular ejection fraction (LVEF), and left ventricular fractional shortening (LVFS).

### 2.14. Real-time polymerase chain reaction

Total RNA extraction was performed using the Total RNA Purification kit (Transgen; Beijing, China). The extracted RNA was then converted into complementary DNA (cDNA) using a transcriptase kit (Transgen; Beijing, China) [15]. The primer sequence used for

**Table 2**  
Primer information.

Gene name	Primer Sequences
GAPDH	F: 5'-TTCAACGGCAGTCAAG-3' R: 5'-TACTCAGCACCAGCATCA-3'
AQP1	F: 5'-CTGATGCTGTGGCTTCTGCTA-3' R: 5'-CTCCTGACTATTCTGCTGCTTCTA-3'
AQP4	F: 5'-TACAGAACCAAGGCGTAGACCG-3' R: 5'-GCTGTCCCTGGAAATGACTGAGA-3'
AQP7	F: 5'-GCATTTTGGCCACCTACCTTCCT-3' R: 5'-CCATTGCTGAAGCCTGTTTGC-3'
AKT	F: 5'-AGAAGGAGGTCATCGTTGCCAAG-3' R: 5'-GCGGTCGTGGGTCTGGAATG-3'
JUN	F: 5'-CGCACCTCCGAGCCAAGAAC-3' R: 5'-GGGTCGGTGTAGTGGTATGTG-3'
VEGFA	F: 5'-TCACCAAAGCCAGCACATAGGAG-3' R: 5'-TCTGCGGATCTTGGACAAACAAATG-3'
IL6	F: 5'-GCCTTCTTGGACTGATGTTGTTG-3' R: 5'-GTCTGTTGTTGGTGTATCCTCTG-3'

gene expression analysis can be found in the Supplementary Materials (Table 2). The gene expression levels related to pyroptosis were quantified using the  $2^{-\Delta\Delta Ct}$  method and normalized to the expression of GAPDH, which served as the internal reference.

### 2.15. Western blotting analysis

Protein extraction was carried out from the aortas of mice in each experimental group, and the protein concentrations were quantified using a bicinchoninic acid (BCA) kit. The samples containing 20  $\mu$ g of protein were subjected to 10 % sodium salt polyacrylamide gel electrophoresis (SDS-PAGE), and the resulting proteins were transferred onto polyvinylidene fluoride (PVDF) membranes (Millipore, IPVH00010). To prevent non-specific binding, the PVDF membranes were blocked for 2 h. Next, the membranes were incubated overnight at 4 °C with diluted primary antibodies (1:1000). After washing the membranes three times with phosphate-buffered saline (PBS), they were further incubated with secondary antibodies (1:5000) for 1 h at room temperature. Finally, the protein expression levels of the different experiment groups were compared and analyzed [16].

### 2.16. Statistical analysis

The data were presented as mean  $\pm$  SD using GraphPad Prism 8.0 (GraphPad Software). Student t-tests were used to analyze differences between two groups. For multiple comparisons, the one-way analysis of variance (ANOVA) test was applied. Spearman's correlation analysis and the  $\chi^2$  test were used to assess the correlation between different gene pairs. The log-rank test was employed to evaluate survival differences. All statistical analyses were two-sided, and a significance level of  $P < 0.05$  was considered statistically significant.

## 3. Results

### 3.1. Screening of active ingredients and prediction of action targets

A comprehensive search in the TCMSP database resulted in the identification of 21 active ingredients, including 3 from sandalwood, 9 from nutmeg, and 9 from jujube. After removing one duplicate item, 20 unique active ingredients remained, and their basic information is shown in Table 3. Further investigation involving the TCMSP and Uniprot databases led to the retrieval of 219 active ingredients corresponding to the target proteins of these 20 active ingredients.

### 3.2. Prediction of potentially useful targets for sanwei sandalwood decoction treatment of heart failure

In our search, we obtained 5898 relevant targets of CHF in the Gene Cards database, 193 in the OMIM database, and 59 in the TTD database. After merging and eliminating duplicates, a total of 5942 relevant targets of CHF were identified. Upon analyzing the interaction between SWTX and CHF targets, we observed 191 intersecting targets, as shown in Fig. 1A,B.

**Table 3**  
Basic information of some potential active components in SWTX.

NO.	ID	Chemical components	OB/ %	DL	Source
1	MOL000358	beta-sitosterol	36.91	0.75	choerospondiatis fructus, myristicae semen
2	MOL001002	ellagic acid	43.06	0.43	choerospondiatis fructus
3	MOL001040	(2R)-5,7-dihydroxy-2-(4-hydroxyphenyl)chroman-4-one	42.36	0.21	choerospondiatis fructus
4	MOL001490	bis [(2S)-2-ethylhexyl] benzene-1,2-dicarboxylate	43.59	0.35	choerospondiatis fructus
5	MOL001736	(-)-taxifolin	60.51	0.27	choerospondiatis fructus
6	MOL000422	kaempferol	41.88	0.24	choerospondiatis fructus
7	MOL004328	naringenin	59.29	0.21	choerospondiatis fructus
8	MOL000096	(-)-catechin	49.68	0.24	choerospondiatis fructus
9	MOL000098	quercetin	46.43	0.28	choerospondiatis fructus
10	MOL007920	meso-1,4-Bis-(4-hydroxy-3-methoxyphenyl)-2,3-dimethylbutane	31.32	0.26	myristicae semen
11	MOL009243	Isoguaiacin	48.78	0.31	myristicae semen
12	MOL009254	galbacin	61	0.53	myristicae semen
13	MOL009255	5-[[2S,3S]-7-methoxy-3-methyl-5-[(E)-prop-1-enyl]-2,3-dihydrobenzofuran-2-yl]-1,3-benzodioxole	53.11	0.4	myristicae semen
14	MOL009259	Kudos	45.06	0.38	myristicae semen
15	MOL009263	saucernetindiol	41.85	0.32	myristicae semen
16	MOL009264	tetrahydrofuroguaiacin B	62.86	0.32	myristicae semen
17	MOL009265	threo-austrobailignan-5	49.49	0.32	myristicae semen
18	MOL000354	isorhamnetin	49.6	0.31	santali albi lignum
19	MOL000006	luteolin	36.16	0.25	santali albi lignum
20	MOL002322	isovitexin	31.29	0.72	santali albi lignum

### 3.3. Construction of “active ingredient-target” network

Using Cytoscape software, we visualized and constructed the “active ingredient-target” network, as shown in Fig. 1C. Among the various compounds, the top active ingredients in the network, ranked by their connectivity with the intersecting targets, were quercetin (122 connections), lignocerol (49 connections), kaempferol (46 connections), naringenin (31 connections), isorhamnetin (27 connections). These active ingredients were identified as key components in the network, crucial for the treatment of CHF. Table 4 provides their basic information.

### 3.4. Protein-protein interaction network

The PPI network was constructed using String database and Cytoscape software, as depicted in Fig. 1D. The network comprises 191 nodes representing protein genes and 3436 edges representing interactions between these protein genes. The maximum degree value in the network is 132, and the average degree value is 36. Among the nodes, there are 21 targets with degrees larger than double the average degree value. In terms of the degree value ranking, the top five protein genes are AKT1, IL6, JUN, CASP3, and VEGFA. These protein genes with high degree values are crucial in the entire network and hold significant positions in the process of treating CHF with SWTX. Further details are provided in Table 5.

### 3.5. Molecular docking

To validate the predicted key active ingredients and key targets, molecular docking was performed using a binding energy criterion of  $\leq -5.0$  kJ/mol (1 kcal/mol = 4.184 kJ/mol). The results of the docking demonstrated that the key active ingredients of SWTX had binding energies much less than  $-5.0$  kJ/mol when docking with the key targets. This indicates that the interaction between the key active ingredients and key targets exhibited good binding activity, confirming the reliability of the study’s predictions. Table 6 presents the results of the molecular docking. Among the key targets, vascular endothelial growth factor A (VEGFA) and the top five active compounds showed particularly strong binding abilities. Fig. 2A illustrates the affinity of each compound with the key targets, along with the binding form of VEGFA with each active ingredient. The compounds with the top 5 binding energies to each target were

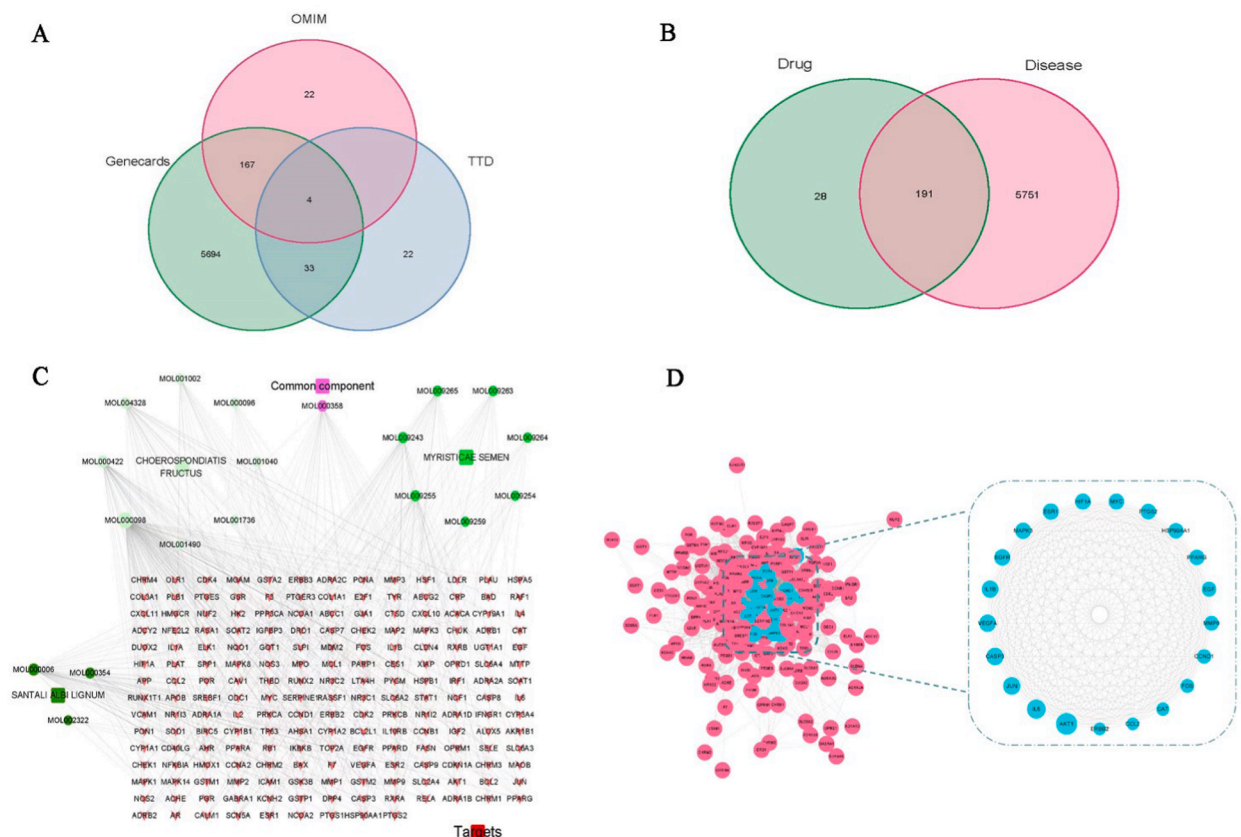
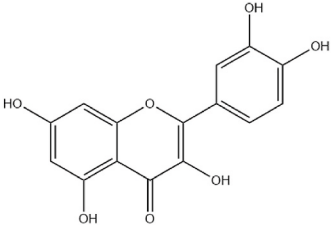
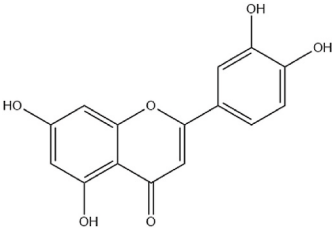
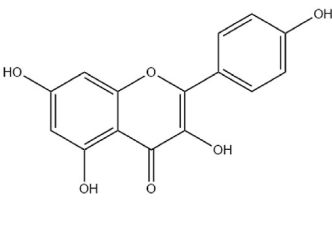
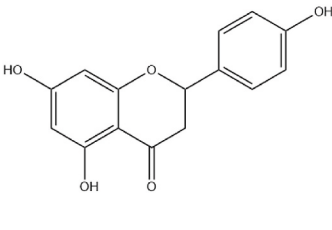
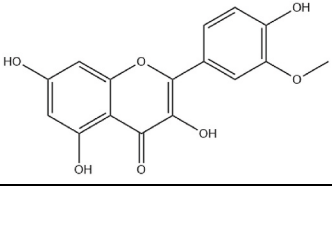


Fig. 1. Network Pharmacology Analysis. A–B: The veen diagram of different databases to find drug ingredients, drug and Disease Targets; C: Sanwei sandalwood decoction “Active Ingredients-Targets” network; D:Protein interaction network.

**Table 4**  
Basic information on key active ingredients.

Chemical components	Degree	Source	Structure
Quercetin	122	choerospondiatis fructus	
Luteolin	49	santali albi lignum	
Kaempferol	46	choerospondiatis fructus	
Naringenin	31	choerospondiatis fructus	
Isorhamnetin	27	santali albi lignum	

**Table 5**  
The basic information on the key targets.

NO.	Abbreviations	English name of target	Degree
1	AKT1	AKT Serine/Threonine Kinase 1	132
2	IL6	Interleukin- 6	116
3	JUN	Jun Proto-Oncogene	106
4	CASP3	Caspase-3	105
5	VEGFA	vascular endothelial growth factor A	104

**Table 6**  
Binding energy of key active components and key targets.

Components	Chemical formula	Relative molecular weight	Target	Energy/(kcal/mol)
Quercetin	C15H10O7	302.24	AKT1	-5.8
			IL6	-4.2
			JUN	-4.8
			CASP3	-6.7
			VEGFA	-7.8
Luteolin	C <sub>15</sub> H <sub>10</sub> O <sub>6</sub>	286.23	AKT1	-6
			IL6	-4.2
			JUN	-5.1
			CASP3	-6.4
			VEGFA	-7.4
Kaempferol	C15H10O6	286.24	AKT1	-5.7
			IL6	-4.0
			JUN	-4.8
			CASP3	-6.3
			VEGFA	-7.6
Naringenin	C <sub>15</sub> H <sub>12</sub> O <sub>5</sub>	272.25	AKT1	-5.7
			IL6	-4.3
			JUN	-4.9
			CASP3	-6.3
			VEGFA	-7.1
Isorhamnetin	C <sub>16</sub> H <sub>12</sub> O <sub>7</sub>	316.26	AKT1	-5.9
			IL6	-4.2
			JUN	-4.7
			CASP3	-6.5
			VEGFA	-7.5

docked to the AQPS target separately using Vina-1.1.1 software, and 3D mapping was performed by Pymol-2.4.0, and the results are shown in Fig. 3A.

### 3.6. Enrichment analysis

During the functional analysis of key targets using GO enrichment, a total of 1665 entries were identified. Among them, 1526 entries represented biological processes, including important functions such as epithelial cell proliferation, response to ROS, cellular response to chemical stress, and response to metal ions. Additionally, 46 entries represented cellular components, encompassing components like RNA polymerase II transcription regulator complex, vesicle lumen, euchromatin, and transcription repressor complex. Moreover, 93 entries were related to molecular functions, including transcription coregulator binding, DNA-binding transcription factor binding, and phospholipase activator activity. These results from the GO analysis highlighted the close relationship between these biological processes, cellular components, and molecular functions and the development of CHF, as presented in Fig. 2B. In the KEGG enrichment analysis of key targets, a total of 132 entries were identified. The pathways mainly included the IL-17 signaling pathway, bladder cancer, TNF signaling pathway, Kaposi sarcoma-associated herpesvirus infection, colorectal cancer, and proteoglycans in cancer, among others, as shown in Fig. 2C.

### 3.7. Kyoto encyclopedia of genes and genomes network

Using Cytoscape software, we visualized the key target-signaling pathway relationship network of SWTX and constructed a “KEGG relationship network diagram”, as depicted in Fig. 3B. In this diagram, circles represent the key targets, while squares represent the KEGG signaling pathways. The analysis revealed that SWTX exerts its therapeutic effects on CHF through the involvement of multiple targets and multiple signaling pathways, highlighting the complexity and multi-faceted nature of the mechanisms by which SWTX treats CHF.

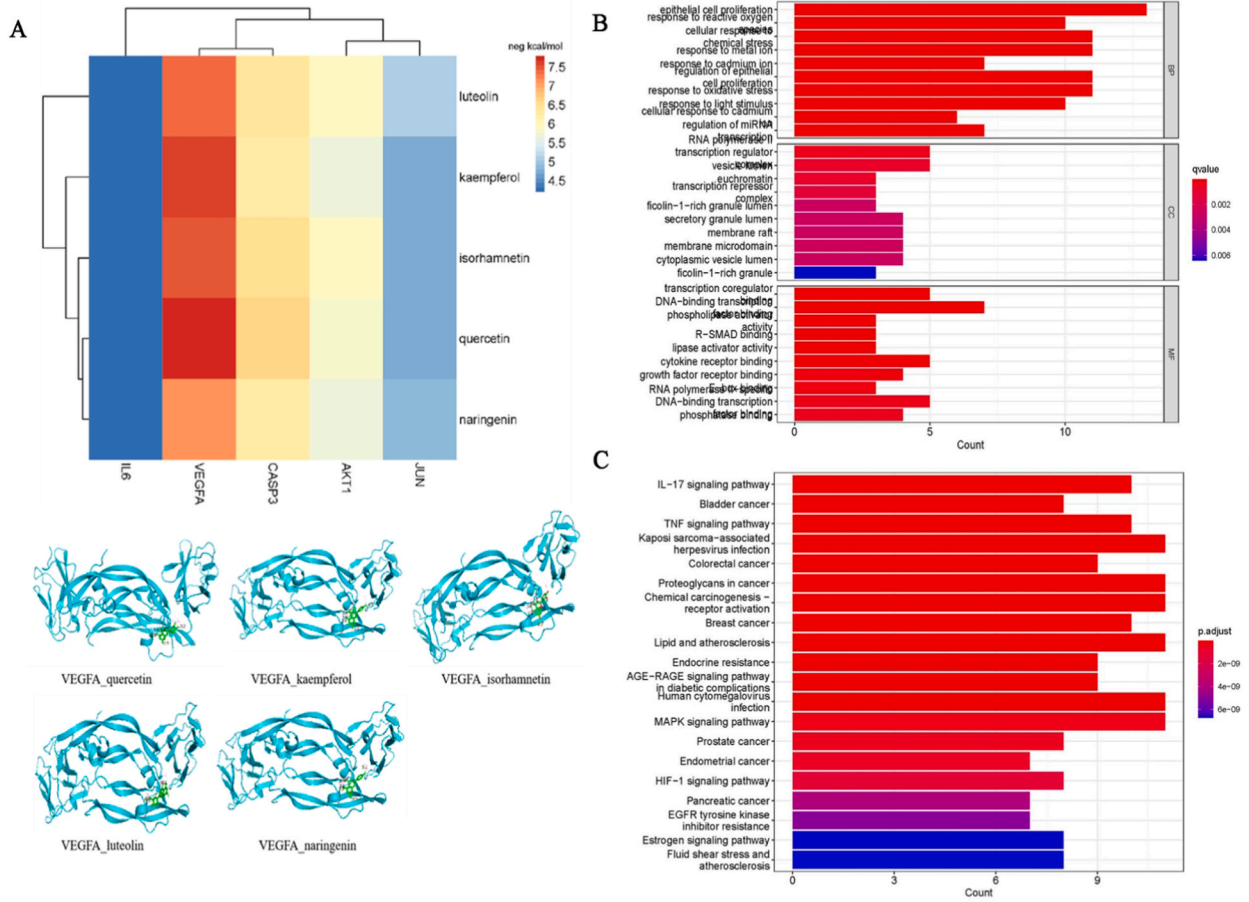


Fig. 2. A:Affinity Heatmap and Molecular Docking Diagram; B:GO enrichment analysis; C:KEGG enrichment analysis.

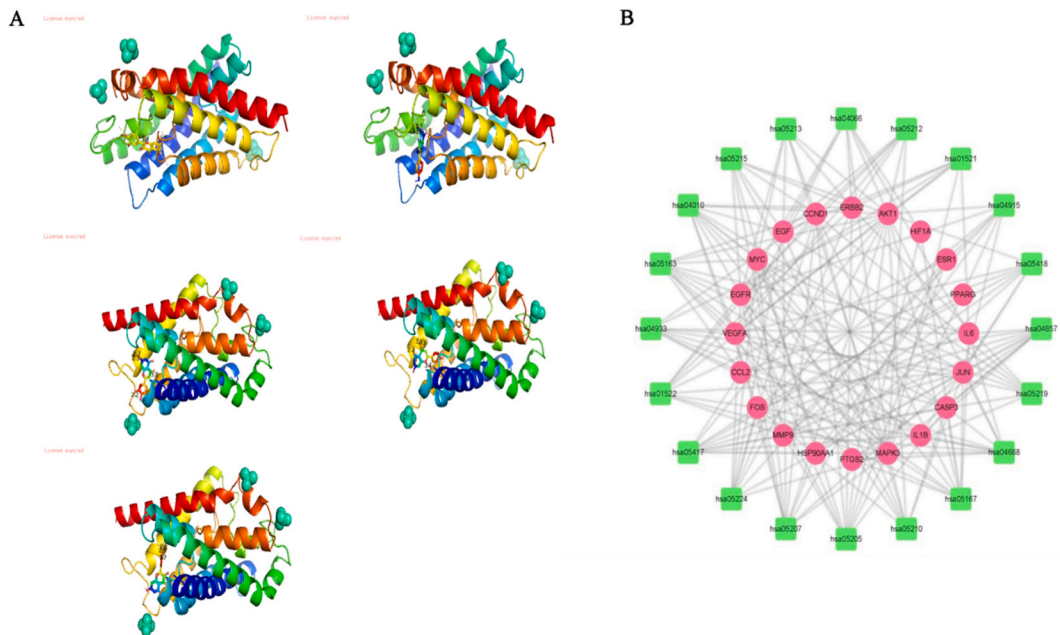


Fig. 3. A:Molecular docking map of AQP proteins; B:KEGG Relationship Network Diagram.

### 3.8. Weight changes

As shown in Fig. 4A, the body weight of rats in the normal group increased steadily over seven consecutive weeks, which is considered a normal and healthy pattern of weight gain. In contrast, the body weight of rats in both the model group and the SWTX group decreased, and they exhibited severe ascites. The difference in body weight before and after the treatment was statistically significant ( $P < 0.05$ ) in both the model group and the SWTX group.

### 3.9. Myocardial histopathological changes

As illustrated in Fig. 5A, the results of HE staining of myocardial tissue revealed distinct differences among the groups. In the normal group, the myocardial fibers of rats were neatly arranged, with most nuclei located in the middle of the cells. The cells were closely connected, and no pathological changes were observed. In the model group, cardiomyocytes exhibited obvious hypertrophy compared to the normal group. The myocardial fibers were arranged in a wavy shape, and some of the fibers showed signs of cracking. The nuclei appeared shifted and solidly shrunken, and the cytoplasm appeared pale. The tissue displayed indications of cell degeneration, necrosis, and interstitial broadening. On the other hand, in the SWTX group, the arrangement of myocardial fibers was denser, and the degree of cell hypertrophy, fracture, degeneration, and necrosis was lower compared to the model group.

### 3.10. Effects of serum cardiac enzymes in rats

The serum levels of CK, CK-MB, and NT-Pro BNP in rats of the model group were significantly increased ( $P < 0.05$ ), indicating the presence of CHF in these rats. Meanwhile, the serum levels of CK, CK-MB, and NT-Pro BNP in rats of the SWTX group were significantly reduced compared to those of the model group in Fig. 5B. This reduction in the biomarker levels suggests that the administration of SWTX had a positive effect on CHF in the rats.

### 3.11. Cardiac ultrasound examination

In comparison to the normal group, the LVEF and LVFS were significantly reduced in the model rats ( $P < 0.05$ ), indicating impaired cardiac function in the rats with CHF. During the drug administration period, LVEF tended to increase ( $P > 0.05$ ), and LVFS increased significantly ( $P < 0.05$ ) in the SWTX group when compared to the model group, as shown in Fig. 4 B,C. These findings suggest that SWTX treatment led to an improvement in the LVEF and enhanced the ejection function of the heart in the rats with CHF.

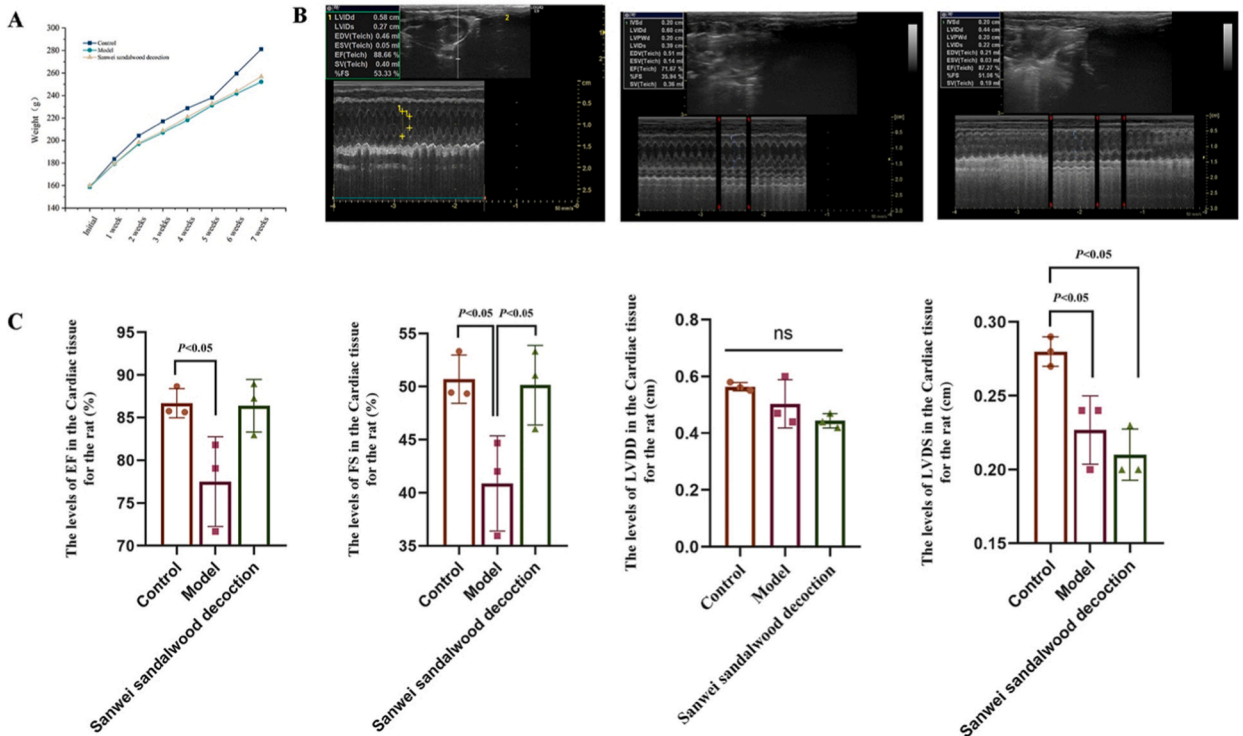


**Fig. 4.** General conditions and cardiac ultrasound analysis in rats A: Rat body weight chart (n = 10); B: Ultrasound picture of the heart (n = 3); C: Indicators of cardiac systolic function (n = 3).

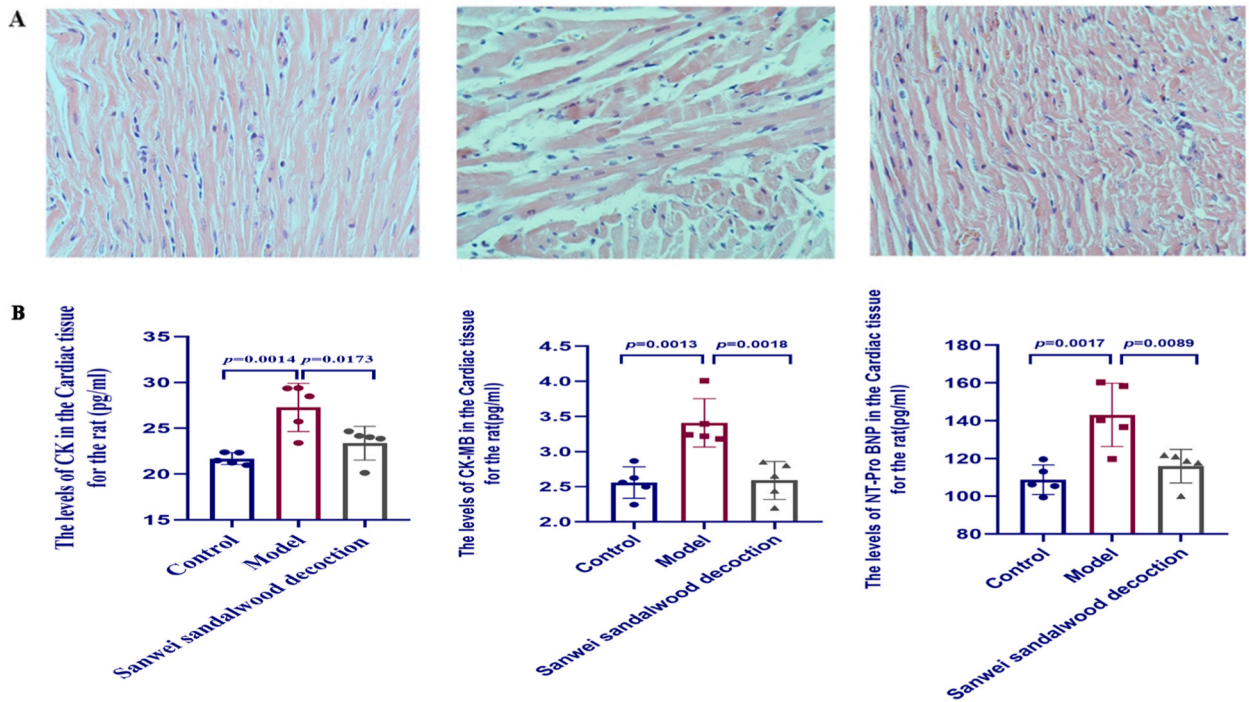


**Fig. 5.** Pathological changes and functional indicators of CHF, A:HE staining of the rats with CHF (n = 3); B:Functional indicators of rats with CHF (n = 5).

In contrast, compared to the normal group, LVSD and LVIDd were reduced in the model group ( $P < 0.05$ ), indicating LV systolic dysfunction in the rats with CHF. During the administration period, the improvement in the above indexes in the rats of the SWTX group was not significant when compared to the model group in Fig. 4B,C. The intervention with SWTX failed to increase the anterior and posterior wall thickness of the left ventricle at the end-diastolic stage in the rats with CHF.

### 3.12. Quantitative reverse transcription-polymerase chain reaction assay of AKT, IL6, JUN, VEGFA and myocardial AQP-1, 4 and 7 mRNA expression

The results of qRT-PCR analysis of myocardial AKT, IL6, JUN and VEGFA mRNA expression showed important findings. The cardiac AKT, IL6 and JUN mRNA expression levels were significantly higher in the model group compared to the normal group, however, the cardiac AKT, IL6 and JUN mRNA expression levels were decreased in the SWTX group compared to the model group, as shown in Fig. 6A. Compared with the normal group, the expression levels of VEGFA mRNA were decreased in the heart of the model group. However, the cardiac VEGFA mRNA expression level was increased in the SWTX group compared to the model group, as shown in Fig. 6A.

The qRT-PCR analysis of myocardial AQP-1,4, and 7 mRNA expression revealed significant findings. When compared to the normal group, the level of cardiac AQP-1,4, and 7 mRNA expression in the model group was significantly increased, indicating elevated expression levels of these AQPs in the heart of CHF rats. However, when comparing the SWTX group to the model group, the level of cardiac AQP-1,4, and 7 mRNA expression in the SWTX group was decreased, as is shown in Fig. 6B. This suggests that the administration of SWTX led to the down-regulation of the highly expressed AQPs-1, 4 and 7 mRNA in the heart of CHF rats.

### 3.13. Myocardial Aquaporins-1,4, and 7 protein expression detected by western blot

The WB analysis of myocardial AQP-1,4, and 7 protein expression yielded significant results. In the heart of rats in the model group, the protein expression levels of AQP-1,4, and 7 were significantly up-regulated, indicating an increase in the levels of the AQPs in response to heart failure. However, in comparison to the model group, the SWTX group showed a significant down-regulation of AQP-1,4, and 7 protein expression levels. This implies that the administration of SWTX led to the down-regulation of the up-regulated AQP-1, AQP-4, and AQP-7 protein expression in the heart of CHF rats in Fig. 7. These findings suggest a potential mechanism through which SWTX may achieve its pre-protective effect against Adriamycin-induced Chronic Heart Failure.

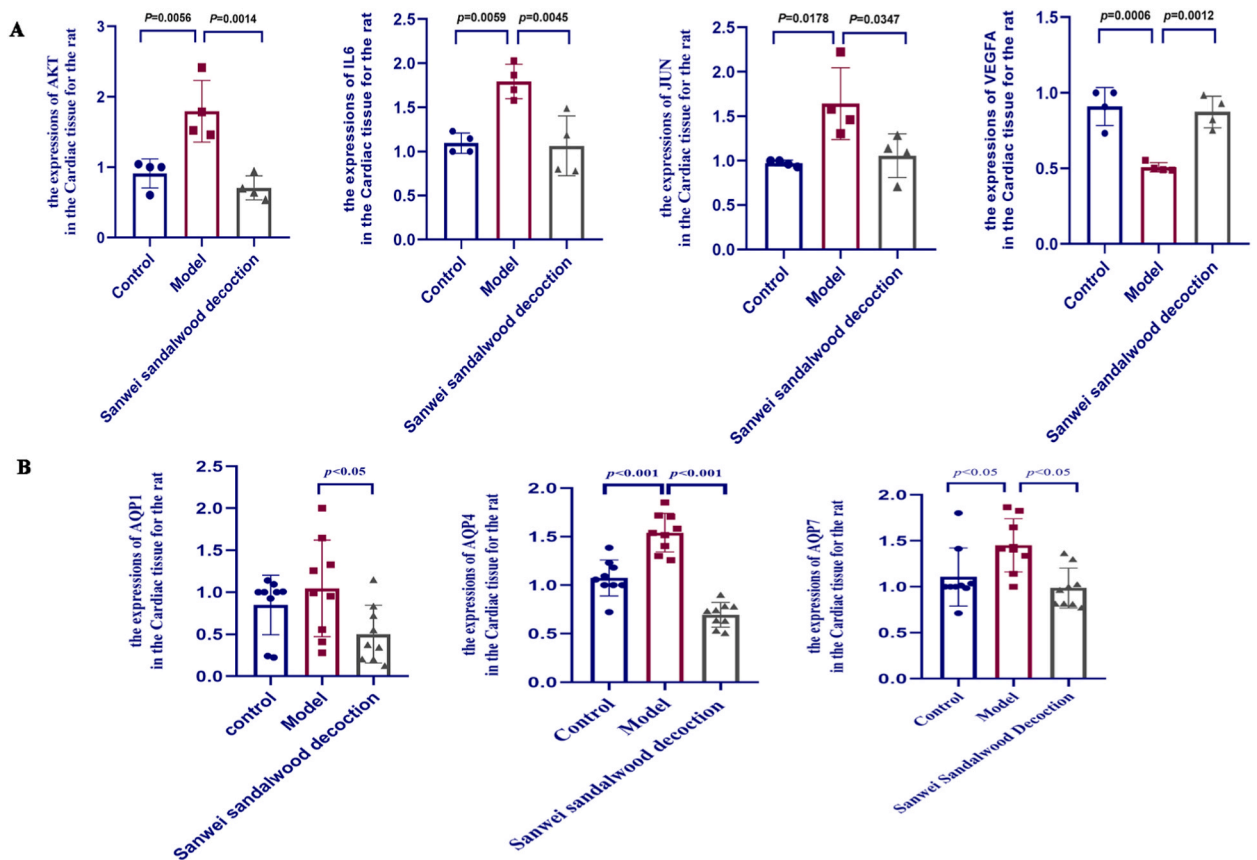


**Fig. 6.** A: The relative expression of AKT, IL6, JUN and VEGFA mRNA of all groups in the rats with CHF (n = 4); B: The relative expression of AQP1, AQP4 and AQP7 mRNA of all groups in the rats with CHF (n = 9).

#### 4. Discussion

In this study, we identified 20 active ingredients present in SWTX and their corresponding targets, which amounted to 219 target proteins. Additionally, we collected 3941 disease-related targets associated with CHF. By taking the intersection of these target sets, we obtained 175 potential targets that are likely involved in SWTX treatment of IHD. Among these active ingredients, the top five compounds based on their network degree value were quercetin, lignocerosol, kaempferol, naringenin, and isorhamnetin, suggesting that these ingredients may play a key role in treating IHD. Quercetin is believed to exert its effects by down-regulating the expression of calpain. The activation of the calpain pathway can lead to cardiac contractile dysfunction, cytoskeletal damage, and apoptosis [17]. Lignans have the potential to reduce cardiac damage caused by oxidative stress through mechanisms involving enhanced eNOS-mediated Keap1 S-nitrosylation and up-regulating nuclear Nrf2 and Nrf2-associated antioxidant signaling pathways [18]. Kaempferol is thought to protect against CHF by reducing oxidative stress, inflammation, and apoptosis [19]. Naringenin has shown to attenuate myocardial injury in IHD by inhibiting mitochondrial oxidative stress injury through activation of AMPK-SIRT3 signaling, thereby protecting mitochondrial function during ischemia-reperfusion injury [20]. Similarly, isorhamnetin can counteract oxidative stress and cardiomyocyte apoptosis by up-regulating SIRT1 and Nrf2/HO-1 mediated antioxidant signaling pathways [21]. These findings collectively imply that the mechanism of SWTX in treating IHD may be associated with its anti-inflammatory, antioxidant, anti-apoptotic, and mitochondrial protective properties.

By constructing the PPI network, we identified the five protein genes with the highest degree values as MAPK3, MAPK1, JUN, RELA, and AKT1. These genes are likely to be key targets for the treatment of CHF by SWTX. Existing studies have shown that MAPK3 plays a protective role in cardiomyocyte apoptosis [22,23], while the MALAT1/miR-15b-5p/MAPK1 axis influences mTOR signaling to regulate autophagy in endothelial cells, improving cell viability and inhibiting apoptosis to protect endothelial cells and influence the coronary artery disease process [24]. The phosphoinositide-3-kinase-AKT serine/threonine kinase 1 (PI3K-AKT) signaling axis is involved in the regulation of cell metabolism, gene expression, cell survival, and migration in various cells [25]. In the vascular wall, AKT plays a crucial role in the proliferation and migration of cardiovascular endothelial cells, as well as in the regulation of vascular permeability and angiogenesis [26,27]. Based on the above findings, together with Fig. 2, it can be observed that the same drug component corresponds to different therapeutic targets, and different targets can be mapped to the same drug component. This indicates that SWTX exerts its pre-protective effect against Adriamycin-induced Chronic Heart Failure through the principle of

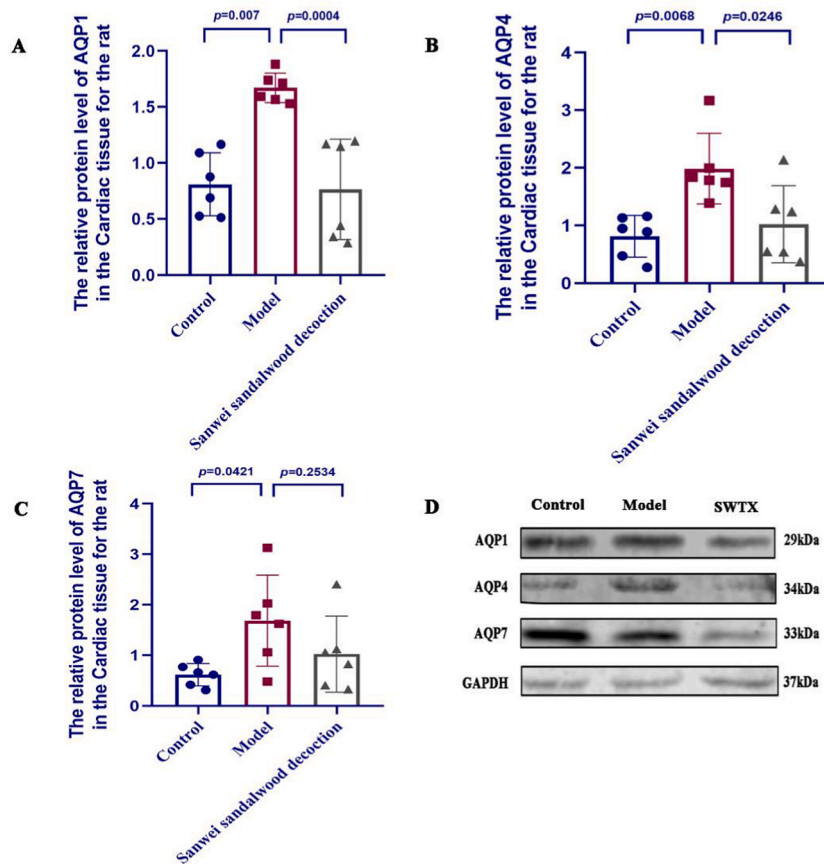


**Fig. 7.** The relative protein level of AQP1, AQP4 and AQP7 of all groups in the rats with CHF(n = 6).A-C:the protein bar graphs; D:protein strip charts.

“multi-components, multi-targets,” involving various functions such as anti-inflammatory, antioxidant, anti-apoptotic, and protection of endothelial cells. The KEGG enrichment analysis revealed that the treatment of CHF with SWTX is associated with multiple pathways. The most closely related pathways include the advanced glycation end-products - receptor for AGEs (AGE-RAGE) signaling pathway, TNF signaling pathway, and 15 other pathways. By combining these results with Fig. 7, it can be inferred that SWTX does not work through a single component, target, or pathway, but rather utilizes a complex “multi-component-multi-target-multi-pathway” network to exert its therapeutic effects in treating CHF.

AQP1 is mainly located in the membranes of human cardiomyocyte and microvascular endothelial cells. Besides its high selectivity for water, AQP1 also facilitates the transport of small molecules such as  $H_2O_2$ , nitric oxide, and carbon monoxide [28]. AQP4, predominantly expressed in the membranes of human cardiomyocytes and vascular endothelial cells, mediates 24-fold more water transport than AQP1 [29]. AQP7 is chiefly involved in cellular energy metabolism and acts as a glycerol channel in cardiomyocytes, providing adenosine triphosphate (ATP) energy substrate for cardiac activity [30,31]. As members of the same family of channel proteins, cardiac AQPs-1,4, and 7 can transport water molecules due to their similar structures, but their unique structures also confer different transport functions. Studies have found that in human hypoxia-reoxygenation cardiomyocytes, the expression levels of AQPs-1,4, and 7 were upregulated compared to the normal group. After pharmacological intervention, downregulation of AQPs-4 and 7 was positively correlated with mitochondrial membrane potential and lysosomal stability, whereas downregulation of AQP1 was positively correlated with cardiomyocyte survival [32]. Currently, the research on AQPs in the heart is limited and mainly focuses on the relationship between abnormal AQP expression and corresponding myocardial diseases [29]. Therefore, the interactions and mechanisms between AQPs-1,4, and 7 isoforms are not yet fully understood. The findings of this study indicate that CHF induced a significant up-regulation of AQPs-1,4, and 7mRNA and protein expression levels in rat hearts, while SWTX treatment down-regulated AQPs-1,4, and 7mRNA and protein expression levels, suggesting that SWTX can regulate the levels of cardiomyocyte AQPs and ameliorate cellular injury.

## 5. Conclusion

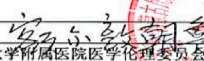
SWTX exhibits the characteristics of “multiple active ingredients, multiple targets, and multiple signaling pathways,” which enable

it to exert a pre-protective effect against Adriamycin-induced CHF by modulating AQPs. Through this experiment, it has been further confirmed that SWTX can down-regulate the expression of AQPs-1,4, and 7 in CHF, leading to reduced myocardial edema and improved cardiac function in rats with CHF. This conclusion is based on the evaluation of myocardial AQPs expression, cardiac function, myocardial injury markers, and myocardial histopathological changes. While this study provides valuable insights, there is still much to be explored in the specific regulatory mechanism of SWTX on AQPs-1,4, and 7. This may involve considering the molecular structure and functional differences of these AQPs, the diverse triggering conditions of AQP signaling pathway subtypes, and the organism's adaptive regulation. It is important to note that this study has certain limitations due to its specific screening conditions. The targets and signaling pathways identified through network pharmacology require further verification through basic clinical trials and pharmacological experiments. By conducting such rigorous follow-up investigations, a more comprehensive understanding of the therapeutic effects and mechanisms of SWTX in treating CHF can be achieved.

**Declarations:** The study was reviewed by the Ethics Committee of the Affiliated Hospital of Inner Mongolia University for Nationalities, and all operations were carried out in accordance with the regulations and in line with animal ethical requirements. The ethical statement is shown below.

伦理审查批件

**内蒙古民族大学附属医院医学伦理委员会**  
**Medical Ethics Committee of Affiliated Hospital of Inner Mongolia University for The Nationalities**  
**伦理审查批件**  
**Approval Notice**

批件号	NM-LL-2022-03-09-02
项目名称	赞丹-3 汤通过网腔钙结合蛋白→心肌阳离子通道介导心肌缺血再灌注心律失常作用研究
申请项目类型	国家自然科学基金
申请人	张青山
申请日期	2022年03月08日
伦理审查方式	
会议审查 <input type="checkbox"/>	快速审查 <input checked="" type="checkbox"/>
伦理审查结论	
<input checked="" type="checkbox"/> 同意 <input type="checkbox"/> 作必要修改后同意 <input type="checkbox"/> 不同意 <input type="checkbox"/> 中止或暂停已批准的试验	
审 核 意 见	根据国家科学技术委员会《实验动物管理条例》、国家食品药品监督管理局《药物临床试验质量管理规范》、国家中医药管理局《中医药临床研究伦理审查平台建设规范》以及世界医学学会《赫尔辛基宣言》的伦理原则，经本伦理委员会审查，本研究为动物实验。研究设计合理，作者承诺遵守动物实验“3R”原则，符合国家实验动物伦理要求，同意申报。
伦理委员会主任委员签字	
伦理委员会	内蒙古民族大学附属医院医学伦理委员会 (盖章)
日期	2022.03.09
备注: 1.临床试验过程中注意事项: 注意对受试者的保护, 严格执行 SAE/SUSAR 的处理, 记录、报告规程及时通知伦理审查委员会, 重新审查, 获得批准后执行。2.试验要求: 遵守 GCP 规定, 严格执行方案, 发现违反方案情况须及时报告伦理审查委员会, 重新审查, 获得批准后执行。3.内容修改要求: 如临床试验方案、知情同意书的任何修改, 应及时通知伦理审查委员会, 重新审查, 获批准后执行。4.暂停/提前终止临床研究的要求: 暂停/提前终止临床研究, 请及时通知伦理审查委员会。5.对完成临床研究要求, 对完成临床研究, 须在完成一个月内, 提交项目结束伦理报告, 供伦理审查委员会审查。6.对临床研究定期跟踪审查要求, 伦理委员会受试者风险程度决定持续审查间隔时间, 确定持续审查的频率, 本试验审查频率为年度审查, 请及时提交持续审查报告, 否则批件失效。7.动物实验注意事项: 应严格遵循实验动物管理条例 (1988年11月14日起施行); 实验动物质量管理办法 (1997年12月11日起施行); 实验动物许可证管理办法 (2002年1月1日起施行)。8.待本项目批准通过后, 请申请人进行伦理会议审查。	

伦理委员会地址及联系电话: 内蒙古民族大学附属医院医学伦理委员会, 电话: 0475-8435512, 内蒙古通辽市霍林河大街1742号 (邮编: 028007)。

## Funding

Inner Mongolia Autonomous Region Self-University Project (GXKT22109) Study on the myocardial protective effect of Mongolian medicine Xin II in rats with viral myocarditis mediated by reticulocyte calcium-binding protein (calumenin);

National Natural Science Foundation of China (82260986) Study on the anti-myocardial ischemia-reperfusion arrhythmia effect mediated by the Mongolian medicine Sanwei Sandalwood Decoction through reticulocyte calcium binding protein → myocardial cation channel.

**Institutional review board statement**

Not applicable.

**Informed consent statement**

Not applicable.

**Data availability statement**

Data is contained within the article.

**CRedit authorship contribution statement**

**Pengfei Hu:** Methodology. **Tingting Bai:** Writing – original draft, Resources. **Zhi Xiu:** Software. **Hujiya:** Methodology. **Ming Li:** Formal analysis. **Qingshan Zhang:** Funding acquisition. **Quan Wan:** Investigation, Funding acquisition, Conceptualization.

**Declaration of competing interest**

The authors declare that they have no known competing financial interests or personal relationships that could have appeared to influence the work reported in this paper.

**Acknowledgments**

The authors thank Quan Wan for assistance with design the article.

**Appendix A. Supplementary data**

Supplementary data to this article can be found online at <https://doi.org/10.1016/j.heliyon.2023.e22718>.

**References**

- [1] M. Songbo, H. Lang, C. Xinyong, et al., Oxidative stress injury in doxorubicin induced cardiotoxicity, *Toxicol. Lett.* 307 (2019) 41–48, <https://doi.org/10.1016/j.toxlet.2019.02.013>.
- [2] G. Akolkar, N. Bhullar, H. Bews, et al., The role of renin angiotensin system antagonists in the prevention of doxorubicin and trastuzumab induced cardiotoxicity, *Cardiovasc. Ultrasound* 13 (1) (2015) 18, <https://doi.org/10.1186/s12947-015-0011-x>.
- [3] Tian Changhai, Gao Lie, Irving H Zuckerman, et al., Extracellular vesicles regulate sympatho-excitation by Nrf2 in heart failure, *Circ. Res.* 131 (8) (2022) 687–700, <https://doi.org/10.1161/CIRCRESAHA.122.320916>.
- [4] Cai Juan, Wang Qi-Ming, Gao Wei, et al., Serum Meteorin-like is associated with weight loss in the elderly patients with chronic heart failure, *J. Cachexia. Sarcopenia. Muscle* 13 (1) (2022) 409–417, <https://doi.org/10.1002/jcsm.12865>.
- [5] A.O. Verkerk, E.M. Lodder, R. Wilders, Aquaporin channels in the heart—physiology and pathophysiology, *Int. J. Mol. Sci.* 20 (8) (2019) E2039.
- [6] T.L. Butlter, C.G. Au, B. Yang, et al., Cardiac aquaporin expression in humans, rats, and mice, *Am. J. Physiol. Heart Circ. Physiol.* 291 (2) (2006) H705–H713, [10.1152/ajpheart.00090.2006](https://doi.org/10.1152/ajpheart.00090.2006).
- [7] R.K. Michael, B. James, Transient transcapillary exchange of water driven by osmotic forces in the heart, *Am. J. Physiol. Heart Circ. Physiol.* 285 (3) (2003) H1317, <https://doi.org/10.1152/ajpheart.00587.2002>.
- [8] A.R. Wright, S.A. Rees, Cardiac cell volume: crystal clear or murky waters? a comparison with other cell types, *Pharmacol. Ther.* 80 (1) (1998) 89–121, [https://doi.org/10.1016/s0163-7258\(98\)00025-4](https://doi.org/10.1016/s0163-7258(98)00025-4).
- [9] Wang Shuyuan, Evgeniy I Solenov, Yang Baoxue, Aquaporin inhibitors, *Adv. Exp. Med. Biol.* 1398 (2023) 317–330, [https://doi.org/10.1007/978-981-19-7415-1\\_22](https://doi.org/10.1007/978-981-19-7415-1_22).
- [10] Zhanting Yang, Effect and Mechanism of Tibetan Medicine Tsantan Sumtang on Right Ventricular Function in Hypoxia-Induced Pulmonary Hypertension Rats, Qinghai University, 2018, <https://doi.org/10.27740/d.cnki.gqhdx.2021.000006>.
- [11] Wujima, Clinical analysis of Guangzao Shuxin Pill in the treatment of chronic myocardial ischaemia, *J. Cardi. Sur.* 7 (1) (2018) 17.
- [12] Yi Zhou, Gerili. Pharmacodynamic and pharmacokinetic research of san wei tan Xiang powder, *Pharm Clin Res* 21 (3) (2013) 261–263.
- [13] Yi Zhou, Based on Proteomics to Study the Protective Effect Mechanism of Tsantan Sumtang on Myocardial Ischemia Rats, SHENGYANG Pharmaceutical University, 2017.
- [14] Y.H. Guo, L.J. Huang, T.T. Di, et al., Fuxin decoction attenuates doxorubicin-induced heart failure in rats via oxidizing suppression and regulating immune responses, *J. Tradit. Chin. Med.* 38 (4) (2018) 579–584.
- [15] Shanshan Li, Yiming Sun, Mengmeng Song, et al., NLRP3/caspase-1/GSDMD-mediated pyroptosis exerts a crucial role in astrocyte pathological injury in mouse model of depression, *J. Clin. Insight.* 6 (23) (2021), e146852, <https://doi.org/10.1172/jci.insight.146852>.
- [16] Pengqi Li, Qiqi Xin, Jiaqi Hui, et al., Efficacy and safety of tongxinluo capsule as adjunctive treatment for unstable angina pectoris: a systematic review and meta-analysis of randomized controlled trials, *Front. Pharmacol.* 12 (2021), 742978, <https://doi.org/10.3389/fphar.2021.742978>.
- [17] P. Allawadhi, A. Khurana, N. Sayed, et al., Isoproterenol-induced cardiac ischemia and fibrosis: plant-based approaches for intervention, *Phytother. Res.* 32 (10) (2018) 1908–1932, <https://doi.org/10.1002/ptr.6152>.
- [18] C. Xiao, M.L. Xia, J. Wang, et al., Luteolin attenuates cardiac ischemia/reperfusion injury in diabetic rats by modulating Nrf2 antioxidant function, *Oxid. Med. Cell. Longev.* (2019), 2719252, <https://doi.org/10.1155/2019/2719252>.
- [19] L. Zhang, Z. Guo, Y. Wang, et al., The protective effect of kaempferol on heart via the regulation of Nrf2, NF- $\kappa$ B, and PI3K/Akt/GSK-3 $\beta$  signaling pathways in isoproterenol-induced heart failure in diabetic rats, *Drug Dev. Res.* 80 (3) (2019) 294–309, <https://doi.org/10.1002/ddr.21495>.

- [20] L.M. Yu, X. Dong, X.D. Xue, et al., Naringenin improves mitochondrial function and reduces cardiac damage following ischemia-reperfusion injury: the role of the AMPK-SIRT3 signaling pathway, *Food Funct.* 10 (5) (2019) 2752–2765, <https://doi.org/10.1039/c9fo00001a>.
- [21] T.T. Zhao, T.L. Yang, L. Gong, et al., Isorhamnetin protects against hypoxia/reoxygenation-induced injury by attenuating apoptosis and oxidative stress in H9c2 cardiomyocytes, *Gene* 666 (2018) 92–99, <https://doi.org/10.1016/j.gene.2018.05.009>.
- [22] Y. Liu, L. Yang, J. Yin, et al., MicroRNA-15b deteriorates hypoxia/reoxygenation-induced cardiomyocyte apoptosis by downregulating Bcl-2 and MAPK3, *J. Investig. Med.* 66 (1) (2018) 39–45, <https://doi.org/10.1136/jim-2017-000485>.
- [23] Tianli Yue, Chuanlin Wang, Juanli Gu, et al., Inhibition of extracellular signal-regulated kinase enhances ischemia/reoxygenation-induced apoptosis in cultured cardiac myocytes and exaggerates reperfusion injury in isolated perfused heart, *Circ. Res.* 86 (6) (2000) 692–699, <https://doi.org/10.1161/01.res.86.6.692>.
- [24] Y. Zhu, T. Yang, J. Duan, et al., MALAT1/miR-15b-5p/MAPK1 mediates endothelial progenitor cells autophagy and affects coronary atherosclerotic heart disease via mTOR signaling pathway, *Aging (Albany NY)* 11 (4) (2019) 1089–1109, <https://doi.org/10.18632/aging.101766>.
- [25] L. Chen, S.Y. Zheng, C.Q. Yang, et al., MiR-155-5p inhibits the proliferation and migration of VSMCs and HUVECs in atherosclerosis by targeting AKT1, *Eur. Rev. Med. Pharmacol. Sci.* 23 (5) (2019) 2223–2233, <https://doi.org/10.26355/eurrev.201903.17270>.
- [26] P. Haslinger, S. Haider, S. Sonderegger, et al., AKT isoforms 1 and 3 regulate basal and epidermal growth factor-stimulated SGHPL-5 trophoblast cell migration in humans, *Biol. Reprod.* 88 (3) (2013) 54, <https://doi.org/10.1095/biolreprod.112.104778>.
- [27] K.M. Nicholson, N.G. Anderson, The protein kinase B/Akt signalling pathway in human malignancy, *Cell. Signal.* 14 (5) (2002) 381–395, [https://doi.org/10.1016/s0898-6568\(01\)00271-6](https://doi.org/10.1016/s0898-6568(01)00271-6).
- [28] S. Al-Samir, D. Goossen, J.P. Cartron, et al., Maximal oxygen consumption is reduced in aquaporin-1 knockout mice, *Front. Physiol.* 7 (2016) 347, <https://doi.org/10.3389/fphys.2016.00347>.
- [29] Qingling Wang, Mechanism Investigation of Xinshuitong Herb Water Extract on Chronic Heart Failure Based on Aquaporin-1,4,7, FUJIAN University of Traditional Chinese Medicine, 2020, <https://doi.org/10.27021/d.cnki.gfjzc>.
- [30] O. Palabiyik, A. Karaca, E. Tastekin, et al., The effect of a high-protein diet and exercise on cardiac AQP7 and GLUT4 gene expression, *Biochem. Genet.* 54 (5) (2016) 731–745, <https://doi.org/10.1007/s10528-016-9753-x>.
- [31] F. Iena, J. Lebeck, Implications of aquaglyceroporin 7 in energy metabolism, *Int. J. Mol. Sci.* 19 (1) (2018) 154, <https://doi.org/10.3390/ijms19010154>.
- [32] Xiao Lu, Study on the Effects of Aqueous Extract of Xinshuitong Compound on Hypoxia-Induced AQPs in Cardiomyocytes, FUJIAN University of Traditional Chinese Medicine, 2015.